expected on the basis of sounding rocket observations (*24*).

In addition to the energy diffusion toward lower energies, the demonstration of the existence of acceleration processes is of particular interest. It implies that the beam-plasma interaction is capable of heating electrons to more than four times the primary beam energy. The observation that the energetic component was present only at high pitch angles is of great importance, as these electrons could be confined much more easily (for instance, by electric fields parallel to the magnetic field) than those with substantial longitudinal energies.

KLAUS WILHELM
WOLFGANG STÜDEMANN
*Max-Planck-Institut für Aeronomie, D-3411 Katlenburg-Lindau, Federal Republic of Germany*
WILLIBALD RIEDLER
*Space Research Institute, Austrian Academy of Sciences, A-8010 Graz*

**References and Notes**

1. A three-axes magnetometer with a time resolution of 1 second was included in the instrument package (experiment 1ES019B). The sensors were mounted close to the spectrometer (1ES019A). During flight, deviations of the magnetic field vector of up to 30° as compared to the nominal model magnetic field were observed, probably due to line and stray currents on the space shuttle and Spacelab. In the absence of final data, no further analysis can be performed at present; analytic models are being worked on.
2. One of the reasons for this restriction is the fact that no flight data other than quick-look information were available for the preparation of this report. As this field of study is relatively new, it is felt that even without having all the supporting information available some conclusions of general interest can be drawn. It must be realized, of course, that important aspects could be overlooked before a detailed analysis of the flight data has been performed.

3. J. R. Winckler, *Rev. Geophys. Space Phys.* **18**, 659 (1980).
4. W. D. Getty and L. D. Smullen, *J. Appl. Phys.* **34**, 3421 (1963).
5. W. Bernstein *et al.*, *Geophys. Res. Lett.* **5**, 127 (1978).
6. J. R. Winckler, in *Artificial Particle Beams in Space Plasma Studies*, B. Grandal, Ed. (Plenum, New York, 1982), pp. 3–33.
7. K. Wilhelm, W. Bernstein, B. A. Whalen, *Geophys. Res. Lett.* **7**, 117 (1980).
8. R. J. Jost, H. R. Anderson, J. O. McGarity, *ibid.*, p. 509.
9. K. Wilhelm, C. Becker, R. Schmidt, Report W84-014, Bundesministerium für Forschung und Technologie, Bonn (1984).
10. B. N. Maehlum, B. Grandal, T. A. Jacobsen, J. Trøim, *Planet. Space Sci.* **28**, 279 (1980).
11. K. I. Gringauz *et al.*, *Ann. Geophys.* **36**, 371 (1980).
12. W. Bernstein, P. J. Kellogg, S. J. Monson, R. H. Holzworth, B. A. Whalen, in *Artificial Particle Beams in Space Plasma Studies*, B. Grandal, Ed. (Plenum, New York, 1982), pp. 35–64.
13. K. Wilhelm, W. Bernstein, P. J. Kellogg, B. A. Whalen, in *Active Experiments in Space*, (ESA-SP 195, European Space Agency, Paris, 1983), pp. 113–120.
14. All space observations available up to now have been made in the backscatter region of the injected beam. Although the measurements presented here fall in the same category, it is hoped that the space shuttle and Spacelab will in the near future provide the facilities required to study the primary beam on a regular basis.
15. As fast reaction times are required, mechanical systems were excluded during the design phase. Instead, a novel electrostatic angular deflection system was devised.
16. The high data collecting capability led to a data rate of more than 200 kbit/sec on a dedicated telemetry channel. A more detailed description of the instrument is given by K. Wilhelm, in *Proceedings of the 21st Convegno Internazionale Scientifico Sallo Spazio* (Rome, 1981), pp. 185–194.
17. The instrument nominally performed more than 100 operational sequences during the Spacelab 1 flight from switch-on 10 hours after launch on 28 November 1983, to shutdown on mission day 9. Since the instrument was encapsulated in a tank with movable cover for protection during takeoff, hottest phases, and landing, several cover activations were required during the flight.
18. Other instrumentation required for the intended investigations includes charged-particle accelerators (experiments 1NS002 and 1ES020) and plasma release systems (1NS002). They are treated in this issue in reports by T. Obayashi *et al.* (*19*) and C. Beghin *et al.* (*22*).
19. T. Obayashi *et al.*, *Science* **225**, 195 (1984).
20. The recorder saturated during the event. However, this does not imply overflow of the count registers.
21. From the fact that these count rate increases did not depend on the switch status of the instrument in both angle and energy and, moreover, did not occur in all azimuthal channels, we conclude that they are related to an as yet unexplained instrumental behavior.
22. C. Beghin *et al.*, *Science* **225**, 188 (1984).
23. Lacking detailed attitude and magnetic field information for the time being, a general conversion from coelevation to pitch angle could not be performed.
24. G. G. Managadze *et al.*, in *Active Experiments in Space* (ESA-SP 195, European Space Agency, Paris, 1983), pp. 161–169.
25. We thank C. Becker, H. Eichel, W. Engelhardt, J. Fein, E. Frank, W. Grill, E. Krahn, W. Neumann, E. Ofner, W. Ramsauer, H. P. Schmidt, R. Schmidt, R. J. Schmidt, K. Schwingenschuh, K. Sommer, and N. Valavanoglou for dedicated work on the technical implementation of the instruments. The project was financially supported by the German Bundesministerium für Forschung und Technologie through grant 01 QV 197-ZA WF-WRK 275/4 and by the Austrian Bundesministerium für Wissenschaft und Forschung as well as the Austrian Academy of Sciences. The assistance of the European Space Agency and National Aeronautics and Space Administration personnel during the development, integration, and mission phases and the cooperation within the Space Plasma Physics Discipline Group of the Spacelab 1 Investigators Working Group as well as the support by the flight crew are greatly appreciated.

27 March 1984; accepted 1 May 1984

# Phenomena Induced by Charged Particle Beams

Abstract. *The effects of electron beam emissions from Spacelab were recorded with onboard diagnostic instruments. The variation of the Spacelab-shuttle potential with respect to the ambient plasma near the scientific air lock was investigated. Data on the waves and instabilities triggered by the electron beams are discussed. Within the electron gyrofrequency and electron plasma frequency range, strong signals were detected by both electric and magnetic antennas during the beam emissions. The frequencies of the emitted waves were compared to the characteristic plasma frequencies to enable mode identification.*

One of the active experiments on Spacelab 1 was designed to investigate phenomena induced by charged particle beams (PICPAB) emitted from the space shuttle. The primary scientific objectives of the PICPAB experiment are related to spacecraft charging, neutralization processes, and beam-plasma interactions. In addition, the experiment was designed to study the transition range between low- and high-power electron beams. Laboratory experiments and experiments in which particle beams were injected into space from rockets had shown that different interaction regimes exist. An initially linear regime extended into intricate nonlinear regimes involving complex mechanisms such as the beam-plasma discharge (*1*). The PICPAB experiment was also designed to begin studies on high-energy ion beams in the ionosphere.

*Instrumentation.* The PICPAB instrumentation consisted of three packages (*2, 3*). The active package, located on the pallet, contained the electron and ion accelerators and diagnostic instruments (particle analyzers and a plasma potential probe). The passive package, deployed outside the scientific air lock by the crew, contained high-frequency (HF) electric (0.1 to 90.9 MHz) and magnetic (0.1 to 11.4 MHz) antennas, a double-sphere electric probe (d-c to 500 Hz), a plasma frequency probe, and an electron temperature probe (ETP). The rack unit, located in the module, was composed of a sweep frequency analyzer connected to the HF antennas and a control unit devoted to mode control, data collection, and main interfacing with the active and passive units and with the general onboard Command and Data Management System. The telemetry rate of the experiment was 1 Mbit/sec. Two basic modes were used and are referred to as "floating" and "nonfloating." In the floating mode the active package was electrically insulated from the Spacelab structure; the package could "float" with respect to the Spacelab potential (limited to ±200 V by design). In the nonfloating mode the active package was electrically grounded to the Spacelab structure, and the net current flowing between the package and the structure was measured. Using one of these two modes, a 5-minute sequence was divided into several modules including low (10 mA) or high (100 mA) beam currents with an electron energy of 8 keV, a pure ion beam (2 mA, 6 keV), two beams of electrons (10 mA) and ions (2 mA), and a neutralized ion beam (ions at 2 mA and electrons at 0 to 4 mA, 100 to 200 eV) (*4*). The PICPAB accelerators were operated

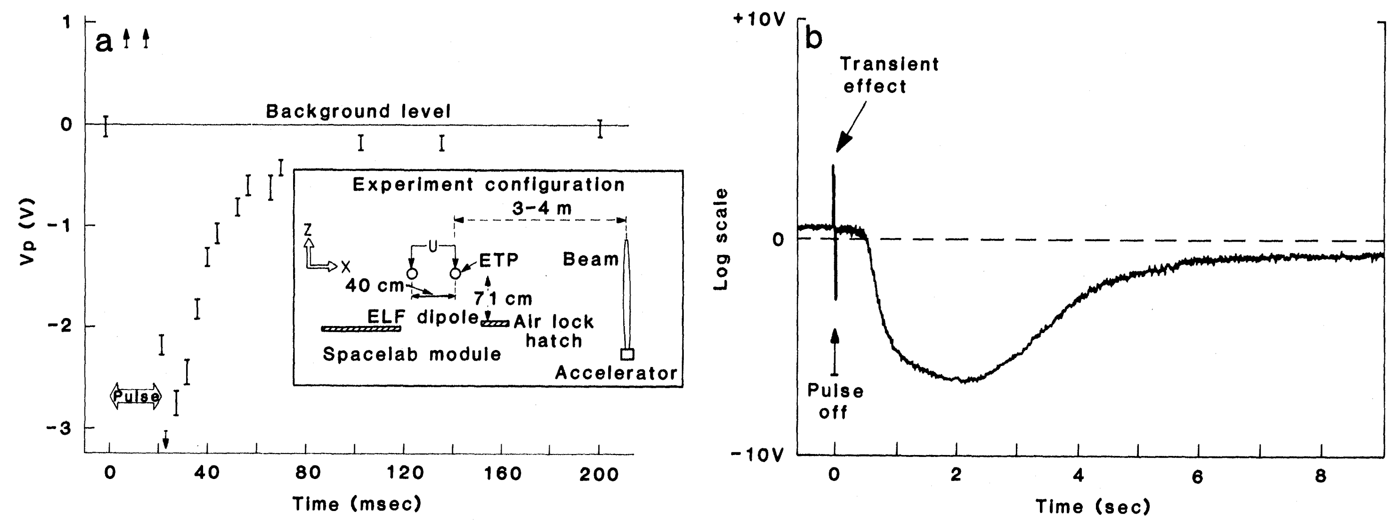


Fig. 1. Time history of neutralization of the shuttle. (a) Shuttle potential variation measured by the electron temperature probe after a pulse (10 mA, 8 kV) emitted by the PICPAB electron accelerator. (b) Potential difference between the two spheres of the axial electric dipole after a SEPAC electron beam accelerator pulse (300 mA, 4 kV).

separately or simultaneously according to a preprogrammed sequence. During a 48-second module the experiment ran in a pulse mode (91 pulses of 20 msec were emitted every 266 msec) and in a modulated mode (91 pulses of 40 msec with 500-Hz modulation were emitted every 266 msec). In addition to the stand-alone operations supported by experiment 1ES019 (*5*), there were operations involving the other two plasma physics experiments, SEPAC (*6*) and AEPI (*7*).

*Neutralization processes.* The shuttle charges positively (negatively) when the electron beam (ion beam) is emitted. This charging, which occurs during beam firing, is expected to take place in a very short time. Such short-time events have not yet been fully analyzed. In this report we concentrate on the neutralization of the shuttle which takes place on a longer time scale after the accelerator pulse. Examples of the observations of the shuttle discharging are presented in Fig. 1. Figure 1a shows the evolution of the shuttle potential with respect to the local plasma potential after a PICPAB low-current electron beam pulse. After an increase of the shuttle potential during the beam pulse, there is a clear overshoot when the beam is switched off. The return to the initial level takes place, in this example, in 200 msec. The evolution of the local d-c electric field along the $x$-axis of the shuttle after a SEPAC electron beam accelerator (EBA) pulse is depicted in Fig. 1b. Our interpretation of the data is as follows. In the local environment of the scientific air lock, where these measurements are performed, surfaces made of different conducting and nonconducting materials are charged at different rates during the

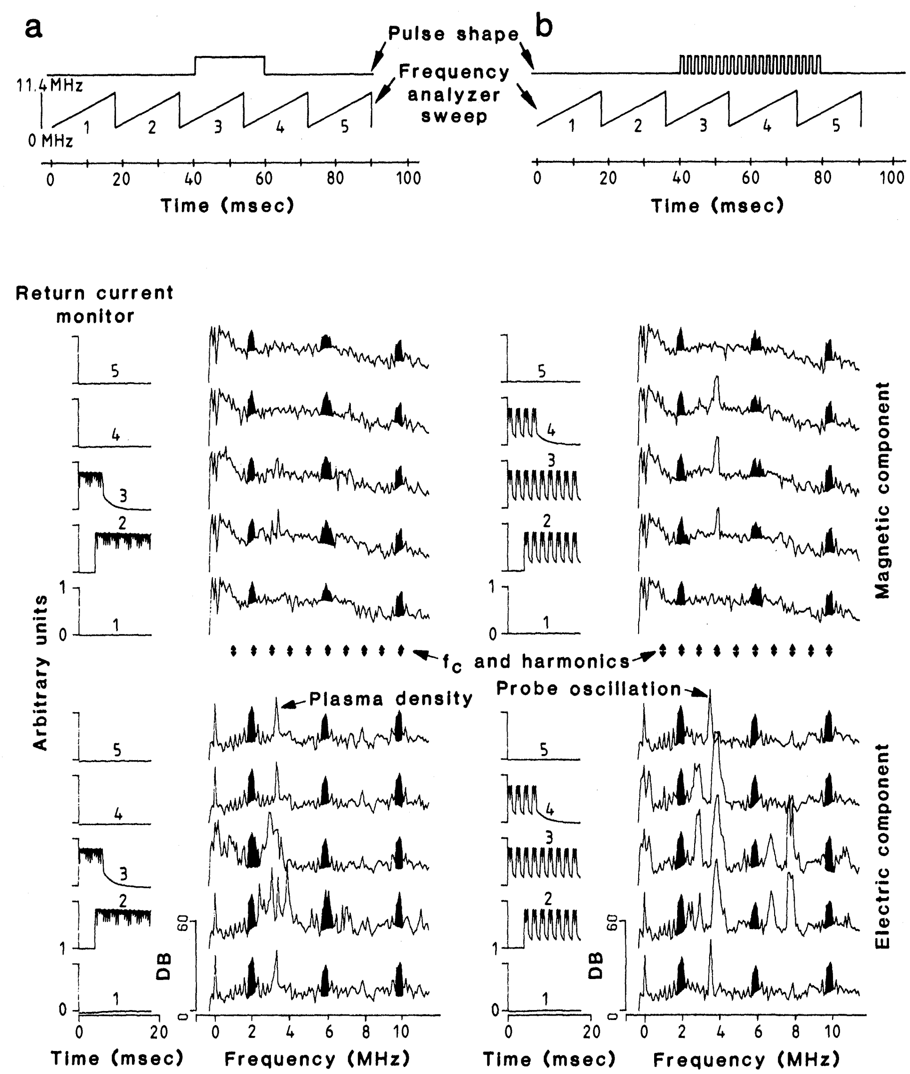


Fig. 2. Frequency spectra recorded before, during, and after a PICPAB electron accelerator pulse (100 mA, 8 kV): (a) in pulse mode (mission elapsed time 0:21:28:50), (b) in modulated mode (2:15:25:48–57). Five consecutive spectra are displayed for the electric and magnetic components. A timing diagram is plotted at the top. Interference lines, filled in in black, are instrumental. The frequency of oscillation of the plasma frequency probe at 3.3 MHz is visible on the electric component spectra. In this example the efficiency of the electron beam in creating instabilities is greater in the modulated than in the pulse mode.

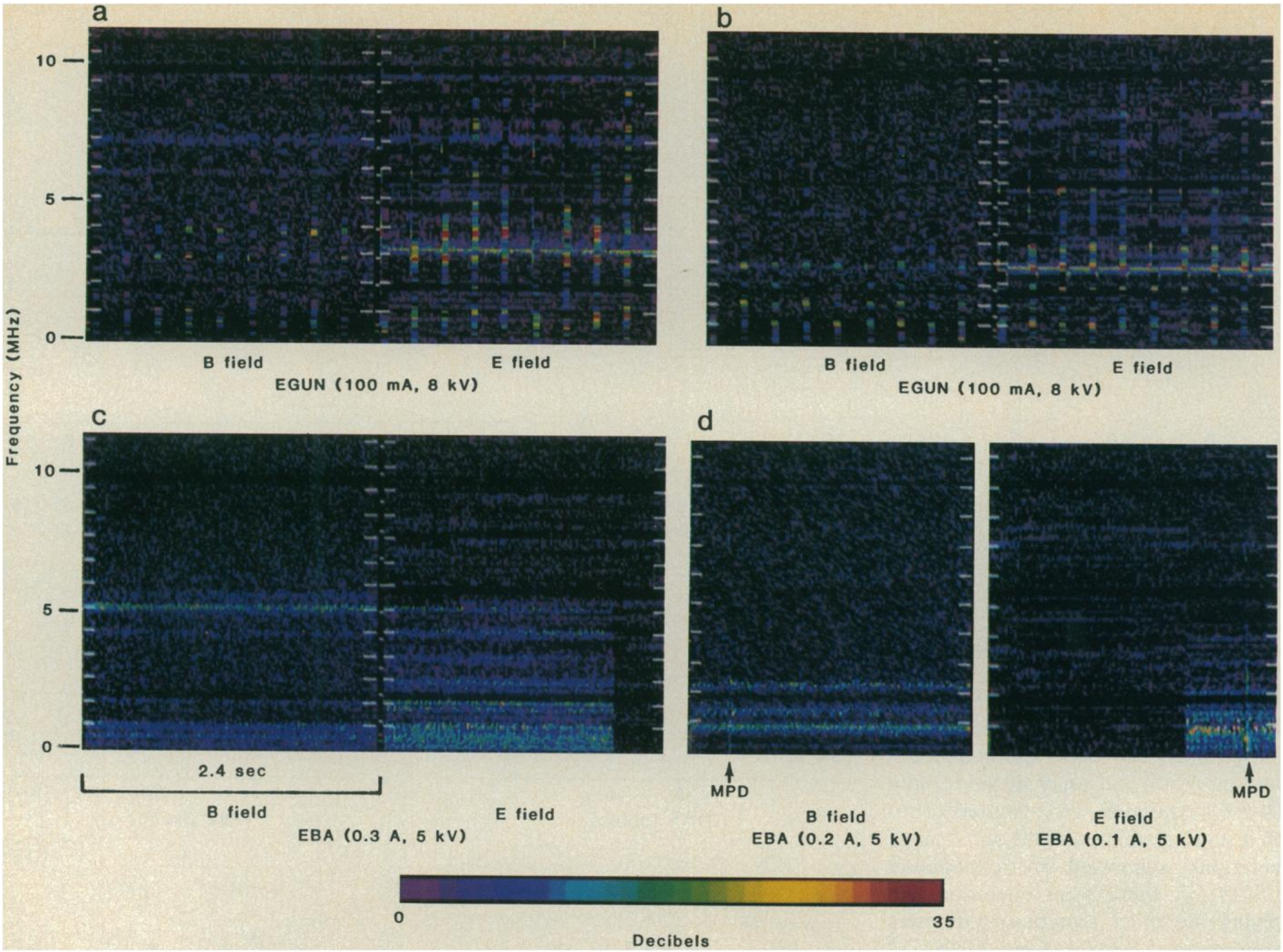


Fig. 3. Color-coded spectrograms for various conditions during the mission (see text). White tick marks indicate the harmonics of the electron gyrofrequency; black tick marks indicate frequency scale, which is the same for all panels. Red corresponds to the highest signal. The spectra are normalized to those obtained during the calibration module at the beginning of each sequence (no beam emission). Data corresponding to the beam emission periods were expanded in time in order to increase readability. Mission elapsed time was: (a) 3:04:31:02–07, (b) 4:04:43:50–55, (c) 2:15:10:33–37, and (d) 2:15:26:10–12 (0.1 A) and 2:15:26:17–19 (0.2 A).

beam pulse. When the beam pulse is switched off, these surfaces discharge at different rates, thus inducing local electric fields. The time constant for the return to the background level may vary from a few milliseconds to several seconds, depending on the level of charging. The parameters that influence the level of charging and the neutralization time constants are now being actively investigated.

An interesting point should be mentioned here. The vehicle is in electrical contact with the plasma through its conductive parts, mainly the engines. Since it moves with a velocity component of up to $v = 7.5$ km/sec perpendicular to the earth's magnetic field ($B$), there is, in the reference frame of the shuttle, a $v \times B$ electric field developing in the plasma at points remote from the engines. This introduces an offset in the value of the local Spacelab-plasma potential measured on the pallet or in the air lock. The offset is 0.45 V/m when the velocity vector is perpendicular to the magnetic field vector ($v = 7.5 \times 10^3$ m/sec, $B = 0.6 \times 10^{-4}$ tesla). As we expect the shuttle (engine) potential to be 1 to 2 V negative with respect to the plasma potential, the local plasma potential measured on the pallet or in the air lock may be either slightly positive or 5 to 6 V negative due to the $v \times B$ offset. This effect must be studied before the beam effect can be analyzed further.

*Wave instabilities.* The plasma wave activity is measured with an electric dipole (0.4 m long) and a magnetic antenna, which are part of the passive package mounted in the air lock. The electric and magnetic signals are analyzed with a swept frequency analyzer (0.1 to 11.4 MHz) in a time-sharing mode. The electric dipole is also part of a mutual impedance probe used in the oscillating mode. The oscillation frequency of this probe is close to the upper hybrid frequency $f_{UH}$ and is a direct measure of the plasma frequency $f_P$ (Eq. 1) and therefore of the plasma density $N_E$ (Eq. 2).

$$f_{UH}^2 = f_P^2 + f_C^2 \quad (1)$$

$$N_E\ (\mathrm{cm}^{-3}) = 0.0121 f_P^2\ (\mathrm{kHz}) \quad (2)$$

Here $f_C$ is the electron gyrofrequency, which is deduced from the magnetic field computed or measured (experiment 1ES019) on board.

A typical wave measurement is shown in Fig. 2. Several consecutive wave spectra, covering a period encompassing a beam pulse, are plotted for both the electric and the magnetic field. These curves display the following features:

1) A broadband emission below $f_C$ in both the electric and the magnetic component. This mode can be identified as the whistler mode.

2) A narrow-band emission near $3f_C$ in the electric component and one near $4f_C$ in both the electric and the magnetic component. Emissions are also seen at higher frequencies, but only in the electric component.

3) A general increase of the noise

background level up to at least 10 MHz in the electric component.

The same wave measurements are also shown in the color spectrograms in Fig. 3a, together with other measurements made under different plasma conditions. Figure 3b shows results of measurements made when the beam was emitted along the magnetic field to within a few degrees. There is a net increase of the wave intensity up to 10 MHz in the electric component. In addition, narrow harmonics of the electron gyrofrequency are excited, as seen in both the electric and magnetic components.

Figure 3c shows the effect of operating the SEPAC electron beam accelerator (5 kV, 0.3 A). The beam was on continuously for 5 seconds. Several narrow-band emissions are observed up to several times $f_C$. In Fig. 3d, which was recorded during another SEPAC electron beam accelerator operation, the effect of the magneto-plasma dynamic arcjet is clearly visible, about 300 msec after the start of the beam pulse, in both the electric and magnetic components.

*Conclusion*. The electron beams injected from the Spacelab pallet produced very clear effects. There were large variations of the shuttle-Spacelab potential with respect to the ambient plasma potential. The relaxation time of the vehicle potential with respect to the plasma potential after the beam is switched off varied from a few milliseconds up to several seconds, the latter result being unexpected. The electrical properties of the materials composing the surface of the spacecraft play an important role, which must be understood before the beam effects can be analyzed. The electron beams also created several instabilities linked to the electron gyrofrequency and its harmonics, and to the plasma and the upper hybrid frequency. In most cases there was a net increase of the electric component of the background noise level in a wide frequency range up to 10 MHz.

C. BEGHIN
*Laboratoire de Physique et Chimie de l'Environnement, 45045 Orleans, France*
J. P. LEBRETON
*Space Science Department, European Space Agency, European Space Research and Technology Centre, 2200 AG Noordwijk, Netherlands*
B. N. MAEHLUM
J. TROIM, P. INGSOY
*Norwegian Defense Research Establishment, Kjeller, Norway*
J. L. MĪCHAU
*Laboratoire de Physique et Chimie de l'Environnement*

**References and Notes**

1. B. Grandal, Ed., *Artificial Particle Beams Utilised in Space Plasma Physics* (Plenum, New York, 1982).
2. C. Beghin, *ESA J.* **3** (No. 2), 123 (1979).
3. ———, in *Active Experiments in Space* (ESA SP-195, European Space Agency, Paris, 1983).
4. The ion accelerator functioned nominally during the first day of the mission until a failure occurred. Ion beam–induced effects will not be discussed in this report.
5. K. Wilhelm *et al.*, *Science* **225**, 186 (1984).
6. T. Obayashi *et al.*, *ibid.*, p. 195.
7. S. Mende *et al.*, *ibid.*, p. 191.
8. The success of this experiment resulted from the work of a number of participants in the PICPAB project. In particular, we thank F. X. Sene, P. Gille, B. Narheim, and U. Gercke, who worked enthusiastically during integrations, flight simulations, and the flight. We also thank Y. Arnal, J.-J. Berthelier, J.-Y. Delahaye, A. Gonfalone, D. Henry, D. Klinge, J. Lavergnat, F. Malerba, N. Overaas, M. Pirre, L. Pomathiod, M. Sylvain, J. F. Karczewski, P. Decreau, and J. M. Illiano. Fruitful discussions with A. Pedersen in the course of the data analysis are acknowledged. We thank the CNES, ESA, NASA, and ERNO personnel for their support during various phases of the project. In particular, we appreciate the support of the ESA Operations Team and the collaboration of the Plasma Physics Discipline Group in the Payload Operations Control Center before and during the mission.

27 March 1984; accepted 10 May 1984

## Atmospheric Emissions Photometric Imaging Experiment

Abstract. *The atmospheric emissions photometric imaging experiment was flown on Spacelab 1 to study faint natural and artificial atmospheric emission phenomena. The instrument imaged optical emission in the region 2000 to 7500 angstroms with a television system consisting of two optical channels, one wide-angle and one telephoto. A third optical channel imaged onto the photochathode of a microchannel plate photomultiplier tube that has 100 discrete anodes. A hand-held image intensifier camera with an objective grating permitted spectral analysis of the earth's airglow and the shuttle glow. Preliminary data show magnesium ion emission features in the lower ionosphere as well as the spececraft glow spectrum.*

One of the scientific objectives of Spacelab 1 was the investigation of the near-earth environment, a region "filled" with space plasmas consisting of charged particles. Spacelab missions are ideally suited for active experiments to study the behavior of these near-earth space plasmas. An active experiment is one in which the environment is perturbed by an artificial stimulus such as a particle beam or a wave injection and the response of the environment is observed. The earth's natural plasma environment or an artificial stimulus interacting with the earth's atmosphere often produces an optical signature such as the aurora or the airglow. The atmospheric emissions photometric imaging (AEPI) experiment was developed to investigate these optical emission signatures from Spacelab.

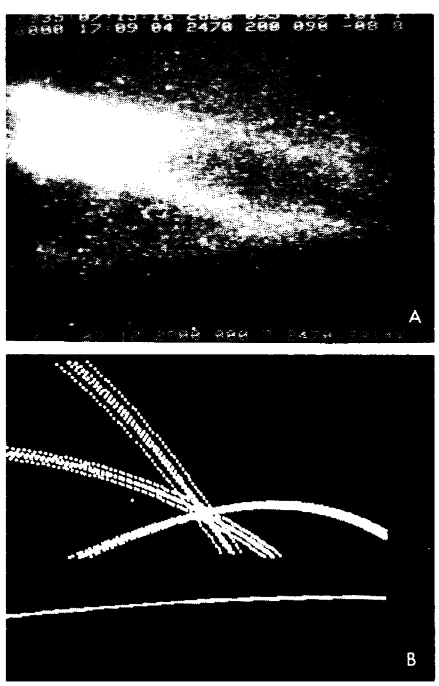


Fig. 1. (A) The 2800-Å filtered images taken by the AEPI television system on mission day 2 at 15 hours, 15 minutes (day 335, 07:15 UT). (B) Magnetic field line plots corresponding to 5 minutes before, during, and 5 minutes after the 2800-Å observations. Field lines are calculated at a distance of 1400 km in front of the observer. The times are: 335:07:10 UT (shallow plot up from left to right), 335:07:15 (shallow plot down from left to right), and 335:07:20 (steep plot down from left to right).

*Instrumentation*. The AEPI instrument (*1*) consists of a low-light-level television camera and an imaging photometer in a unit mounted on a two-axis pointing system located on the Spacelab pallet. It was controlled by a minicomputer and associated hardware located in the manned Spacelab module. The total mass of the AEPI experiment was 168 kg. Power consumption was typically 330 W. The AEPI instrument was developed jointly by Lockheed Missiles and Space Company and NASA–Marshall Space Flight Center with assistance from Boston College.

The sensing head of the AEPI instrument, the detector assembly, consists of two principal parts: a dual-channel, low-light-level television system (LLLTV) and a photon counting array (PCA). The system includes appropriate optical filters to provide spectral sensitivity and